



Technical Report HCSU-115

2022–2024 STATUS AND TRENDS OF THE PALILA (*LOXIOIDES BAILLEUI*)

Noah Hunt¹, Chauncey K. Asing², Lindsey Nietmann³, Paul C. Banko⁴,
and Richard J. Camp⁴

¹Hawai'i Cooperative Studies Unit, University of Hawai'i at Hilo, 200 W. Kawili Street,
Hilo, HI 96720

²University of Hawai'i at Mānoa, Pacific Cooperative Studies Unit, 3190 Maile Way,
St John 408, Honolulu, HI 96822

³Division of Wildlife Conservation, Alaska Department of Fish and Game, 333 Raspberry
Road, Anchorage, AK 99518

⁴U.S. Geological Survey, Pacific Island Ecosystems Research Center,
P.O. Box 44, Hawaii National Park, HI 96718

Hawai'i Cooperative Studies Unit
University of Hawai'i at Hilo
200 W. Kawili St.
Hilo, HI 96720
(808) 933-0706

May 2025



UNIVERSITY
of HAWAII®
HILO

Citation: Hunt, N. J., C. K. Asing, L. Nietmann, P. C. Banko, and R. J. Camp. 2025. 2022–2024 Status and trend of the palila (*Loxioides bailleui*). Hawai'i Cooperative Studies Unit Technical Report HCSU-115. University of Hawai'i at Hilo. 22 pages. <https://hdl.handle.net/10790/5398>

This product was prepared under Cooperative Agreement CAG21AC10163 for the U.S. Geological Survey Pacific Island Ecosystems Research Center.

Any use of trade, firm, or product names is for descriptive purposes only and does not imply endorsement by the U.S. Government.

TABLE OF CONTENTS

| | |
|------------------------------------|-----|
| List of Tables | iii |
| List of Figures | iii |
| Abstract..... | 1 |
| Introduction | 1 |
| Methods..... | 2 |
| Study Area & Bird Sampling | 2 |
| Abundance Estimation..... | 4 |
| Trend Detection..... | 6 |
| Sampling Condition Evaluation..... | 7 |
| Results..... | 7 |
| Abundance Estimation..... | 7 |
| Trend Detection..... | 8 |
| Sampling Condition Evaluation..... | 8 |
| Conclusions | 14 |
| Acknowledgements..... | 15 |
| Literature Cited | 16 |

LIST OF TABLES

| | |
|---|----|
| Table 1. Number of transects and stations sampled by year inside and outside the core survey area from 1998 to 2024 on Mauna Kea, Island of Hawai'i. | 4 |
| Table 2. Results of fitting 12 detection function models to the 1998–2024 palila distance histogram. | 9 |
| Table 3. Annual palila detections and population estimate parameters from 1998–2024..... | 11 |

LIST OF FIGURES

| | |
|---|----|
| Figure 1. Palila survey area for the 2022–2024 surveys. | 3 |
| Figure 2. Survey years grouped by the similarity of their parameter coefficients into five blocks. | 5 |
| Figure 3. Palila detected per visit across 2022–2024 surveys. | 8 |
| Figure 4. Hazard-rate detection function and probability density of the best-fit detection model. | 10 |
| Figure 5. Annual palila population estimates from 1998 through 2024 inside the core survey area on the western slope of Mauna Kea. | 12 |
| Figure 6. State-space model estimates of palila abundance over multiple time spans—the most recent 5, 10, and 15 years, and the full series from 1998 to 2024. | 13 |
| Figure 7. Violin plots displaying the distribution of weather covariate values for each survey year..... | 14 |

ABSTRACT

Palila (*Loxioides bailleui*) are critically endangered Hawaiian honeycreepers specializing on the seedpods of māmane (*Sophora chrysophylla*) and restricted to Mauna Kea volcano on the Island of Hawai'i. A previous analysis of survey data estimated an 89% population decline between 1998 and 2021. Using the most recent annual survey data from 2022, 2023, and 2024, we report updated annual population estimates and trends since 1998. The 2022 population estimate was 367–742 birds (point estimate: 545); the 2023 population estimate was 374–842 birds (point estimate: 596); and the 2024 population estimate was 412–970 birds (point estimate: 666). Our estimates for survey years prior to 2022 were within the confidence intervals of the estimates from the previous analysis. Our models likewise showed a population fluctuating between 4,000 and 6,800 birds from 1998 to 2005 (except for an unusually low estimate in 2000), and then a steep decline through 2010. For the next decade, palila abundance fluctuated between 776 and 1,346 birds, before declining again in 2021 to 679 birds. From 1998 to 2024, the population declined by >90% or 203 birds/year, with very strong statistical evidence of an overall downward trend.

INTRODUCTION

Palila (*Loxioides bailleui*) are critically endangered, finch-billed Hawaiian honeycreepers (family Fringillidae), and the last of the seed specialists in this adaptive radiation remaining within the main Hawaiian Islands. Approximately 2.84 million years ago, palila diverged from the ancestors of the Laysan finch (*Telespiza cantans*) and Nihoa finch (*Telespiza ultima*; Lerner *et al.* 2011), and colonized the dry forests of at least Kaua'i, O'ahu, and the Island of Hawai'i (Olson and James 1982, Burney *et al.* 2001, Banko *et al.* 2020), based on subfossil and historical evidence. They evolved to feed almost exclusively upon the seed pods of endemic māmane (*Sophora chrysophylla*; family Fabaceae), which contain compounds toxic to most other species (Banko *et al.* 2002a). Their dependence on māmane seeds has increased markedly compared to their reconstructed diet showing greater exploitation of caterpillars more than a century ago (Van Houtan *et al.* 2024). Today, they are found only in subalpine dry forest on the southwest slope of Mauna Kea, where habitat conditions are rapidly changing due to climate change and invasive species, especially feral ungulates (Banko *et al.* 2013, 2014).

By the late 18th century, when palila were found only on the Island of Hawai'i, Europeans introduced cattle (*Bos taurus*), sheep (*Ovis aries*), and goats (*Capra hircus*), which subsequently browsed and degraded much of the remaining Hawaiian māmane-naio (*Myoporum sandwicense*; family Scrophulariaceae) forest (Scowcroft 1983, Hess *et al.* 1999). Palila subsequently vanished from the slopes of Hualālai and Mauna Loa. A nearly successful attempt to eradicate feral livestock from Mauna Kea in the 1930s and 1940s evolved into a sustained game management plan by the 1950s (Juvik and Juvik 1984). Feral sheep were allowed to proliferate and were even augmented by mouflon (*O. aries musimon*) in the 1960s (Juvik and Juvik 1984), which reversed any recent forest recovery (Reddy *et al.* 2012). This precipitated a series of lawsuits which eventually obligated the State of Hawaii to remove feral livestock from Palila Critical Habitat (Juvik and Juvik 1984).

Reducing feral ungulate populations after 1980 promoted a moderate level of māmane regeneration (Hess *et al.* 1999, Reddy *et al.* 2012). However, palila numbers oscillated throughout the 1980s and 1990s, likely tracking with droughts affecting the annual variation in māmane seed pod output (Jacobi *et al.* 1996, Lindsey *et al.* 1997, Gray *et al.* 1999). Palila then started to markedly decline around the turn of the 21st century, steadily from 2005 until 2010,

and more slowly afterward, with population estimates reaching an all-time low in 2021 (Leonard Jr. *et al.* 2008, Banko *et al.* 2009, Gorresen *et al.* 2009, Banko *et al.* 2013, Genz *et al.* 2022). Existential threats, including drought, fire, invasive mammalian predators, especially feral cats (*Felis catus*), invasive weeds, māmane fungal pathogens, and introduced insects which deplete food resources, continue to threaten palila survival and reproduction (Hughes *et al.* 1991, D'Antonio and Vitousek 1992, Jacobi *et al.* 1996, Hess *et al.* 1999, Gardner and Trujillo 2001, Hess *et al.* 2004, Oboyski *et al.* 2004, USFWS 2006, Banko *et al.* 2009, Banko *et al.* 2013, Banko *et al.* 2020).

Occupying only about 5% of their historical range (Scott *et al.* 1984, Banko *et al.* 2013), palila follow the seasonal abundance of māmane pods along an elevational gradient on the western slope of Mauna Kea (Jacobi *et al.* 1996, Hess *et al.* 2001, Banko *et al.* 2002b). While palila distribution shifts with their primary food source, their seasonal ranges overlap extensively, therefore the area surveyed annually each winter provides a stable and representative basis for evaluating population abundance and trends. Palila nesting season follows annual surveys and coincides with peak māmane production (March–September; Banko and Farmer 2014). Recurring drought and a trend toward drier climatic conditions, compounded by feral ungulate browsing, have reduced māmane seed production and, consequently, the palila population (Banko *et al.* 2013).

This report updates the population status and trends for palila since 1998 with new data from the 2022, 2023, and 2024 annual surveys. While annual palila surveys have been conducted since 1980 (Scott *et al.* 1984), additional transects were added to the original Hawaiian Forest Bird Survey area in 1998 to improve population estimation precision and provide a more comprehensive coverage of palila distribution during the survey period (Johnson *et al.* 2006). Consequently, our estimates are restricted to the timespan of the larger survey effort (1998 through 2024).

METHODS

Study Area & Bird Sampling

Since 1980, 95% of the palila population inhabited a 64.4 km² area on the southwestern slope of Mauna Kea, within the federally designated Palila Critical Habitat (Scott *et al.* 1984, USFWS 2006, Banko *et al.* 2013, Camp *et al.* 2014; Figure 1). We refer to this area hereafter as the “core survey area.”

During 25 January–17 February 2022, 2–13 February 2023, and 30 January–15 February 2024, point-transect distance sampling was conducted on Mauna Kea to estimate palila abundance and range. For all three years, 13 bird survey transects inside the core survey area (transects 101–108 and 122–126; Figure 1) were surveyed one or more times. In addition to the core survey area, supplemental transects to the east of the core range were surveyed in all three years to look for possible range expansion. These included transects 109–121 in 2022, 109 in 2023, and 109 and 110 in 2024. Within the Ka'ōhe mitigation area (Banko *et al.* 2009; Figure 1), surveys were conducted on supplemental sampling points (also called stations) in the lower portions of transects 102, 124, and 125 in 2022, and the lower portions of transects 101, 102, 124, and 125 in 2023 and 2024.

Within the core survey area, the 2022 survey consisted of 417 counts at 417 stations, the 2023 survey consisted of 415 counts at 408 stations, and the 2024 survey consisted of 396 counts at 391 stations (Figure 1, Table 1). The adjacent, supplemental stations outside of the core survey area were each counted once in 2022 (325 counts), 2023 (78 counts), and 2024 (89 counts).

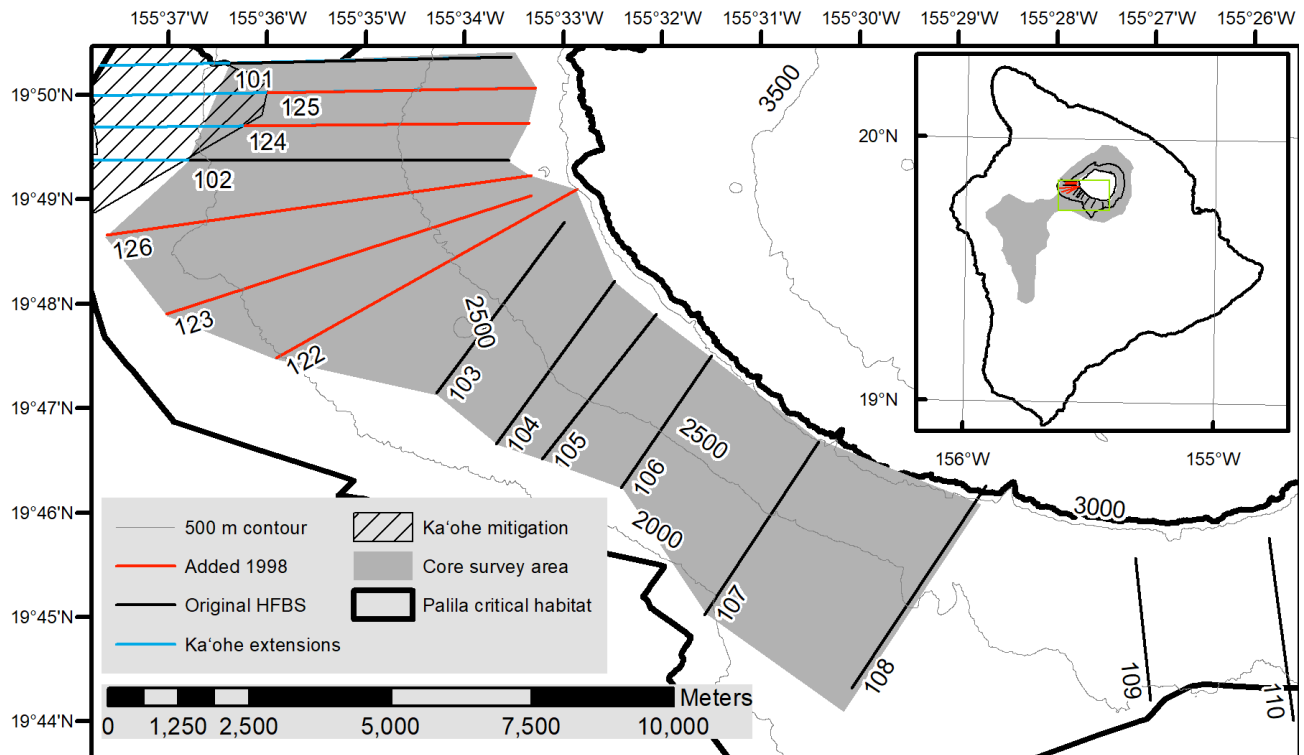


Figure 1. Palila survey area for the 2022–2024 surveys. The area used to estimate palila population abundance is demarcated by the shaded region. Lines depict the original Hawaiian Forest Bird Survey (HFBS) transects (black) plus those added in 1998 (red), including supplemental survey effort on transects 109 and 110. Supplemental transect extensions into the Ka'ohe mitigation area are blue. The inset map shows the transects, Palila Critical Habitat (black line), and historical palila range (gray polygon) on the Island of Hawai'i. Base map from World Geodetic System 1984 (WGS84) zone 5; coastline from U.S. Geological Survey's National Elevation Dataset (U.S. Geological Survey 2018; contour interval 500 m).

Since the introduction of transects 122–126 in 1998 palila abundance estimates were produced by U.S. Geological Survey (USGS) and partners (Camp and Banko 2012; Camp *et al.* 2014, 2016; Genz *et al.* 2018). Prior to 2008, surveys were conducted mountain-wide, but the lack of detections outside the southwestern slope led to focusing effort on the core survey area with the intent to survey the entire mountain every five years starting in 2012 (David L. Leonard Jr., State of Hawaii, Department of Land and Natural Resources Division of Forestry and Wildlife, oral comm., 2012). Most forest bird surveys in the Hawaiian Islands last eight minutes (Camp *et al.* 2009), however, palila counts last six minutes because their woodland habitat is more open than mesic and wet forest habitats, allowing for easier and more rapid detection. Counts commenced at sunrise and continued up to four hours (approximately 11:00 HST). During each count, trained and calibrated observers recorded the species, detection type (heard, seen, or both), and horizontal distance of each bird from the observer. Time of sampling and weather conditions (cloud cover, rain intensity, wind strength, and wind gust strength [hereafter gust strength]) were also recorded, and surveying was postponed when conditions hindered the ability to detect birds (wind and gust strengths >20 kilometers per hour [kph] or heavy rain).

Table 1. Number of transects and stations sampled by year inside and outside the core survey area from 1998 to 2024 on Mauna Kea, Island of Hawai'i.

| Year | Inside core survey area | | | Outside core survey area | | |
|------|-------------------------|----------|--------|--------------------------|----------|--------|
| | Transects | Stations | Counts | Transects | Stations | Counts |
| 1998 | 12 | 355 | 358 | 14 | 186 | 186 |
| 1999 | 13 | 417 | 418 | 14 | 192 | 206 |
| 2000 | 13 | 418 | 428 | 17 | 224 | 224 |
| 2001 | 13 | 416 | 417 | 17 | 223 | 223 |
| 2002 | 13 | 417 | 417 | 20 | 270 | 270 |
| 2003 | 13 | 404 | 410 | 20 | 258 | 258 |
| 2004 | 13 | 399 | 399 | 18 | 244 | 244 |
| 2005 | 13 | 403 | 428 | 21 | 352 | 352 |
| 2006 | 13 | 386 | 386 | 21 | 353 | 353 |
| 2007 | 13 | 408 | 412 | 20 | 253 | 253 |
| 2008 | 12 | 387 | 387 | 3 | 53 | 53 |
| 2009 | 13 | 416 | 416 | 0 | 0 | 0 |
| 2010 | 13 | 415 | 420 | 0 | 0 | 0 |
| 2011 | 13 | 411 | 432 | 0 | 0 | 0 |
| 2012 | 13 | 420 | 843 | 24 | 426 | 426 |
| 2013 | 13 | 418 | 889 | 0 | 0 | 0 |
| 2014 | 13 | 407 | 817 | 7 | 115 | 169 |
| 2015 | 13 | 420 | 839 | 4 | 63 | 125 |
| 2016 | 13 | 420 | 837 | 5 | 79 | 97 |
| 2017 | 13 | 420 | 825 | 22 | 367 | 421 |
| 2018 | 13 | 419 | 419 | 6 | 97 | 98 |
| 2019 | 13 | 417 | 420 | 7 | 83 | 83 |
| 2020 | 13 | 419 | 421 | 2 | 23 | 23 |
| 2021 | 13 | 420 | 422 | 5 | 74 | 74 |
| 2022 | 13 | 417 | 417 | 22 | 325 | 325 |
| 2023 | 13 | 408 | 415 | 5 | 78 | 78 |
| 2024 | 13 | 391 | 396 | 6 | 89 | 89 |

Abundance Estimation

Distance analysis fits a detection function to estimate the probability of detecting a bird at a given distance from the observer, with the probability of detection decreasing with increasing

distance. Previous analysis of palila surveys (Genz *et al.* 2022) demonstrated that the probability of detection was affected not only by distance but also by covariates such as detection type, sampling conditions, time of day, and survey year. A detection function was therefore fitted to models with and without these covariates as sample size post-stratification allowed (Thomas *et al.* 2010). Modeling covariates gives better precision, assuming the same key function for all factors (Buckland *et al.* 2015). Pooling covariates that have a similarly shaped detection function, based on similar coefficient values, can improve model fit, substantially reduce computation time, and can further increase precision. Detection type was evaluated as heard only (detection type = 1) versus seen first (detection type = 2) or heard first and then seen (detection type = 4), where seen first detections were pooled with heard then seen detections (detection type 1 versus 2 + 4). For weather conditions, wind strength was pooled into counts with light wind (Beaufort scale 0–1) or heavy wind (2 or greater). Gust strength was similarly pooled into counts with light gusts or heavy gusts using the same scale. We also included time since the earliest survey start, as time of day may affect bird activity levels and therefore detectability. Survey years were included both as discrete factors and as five blocks of pooled years, based on similar parameter coefficients (Figure 2). With each additional year of data, estimates of these effects become more precise, and the improved detection function may cause population estimates of previous years to change slightly.

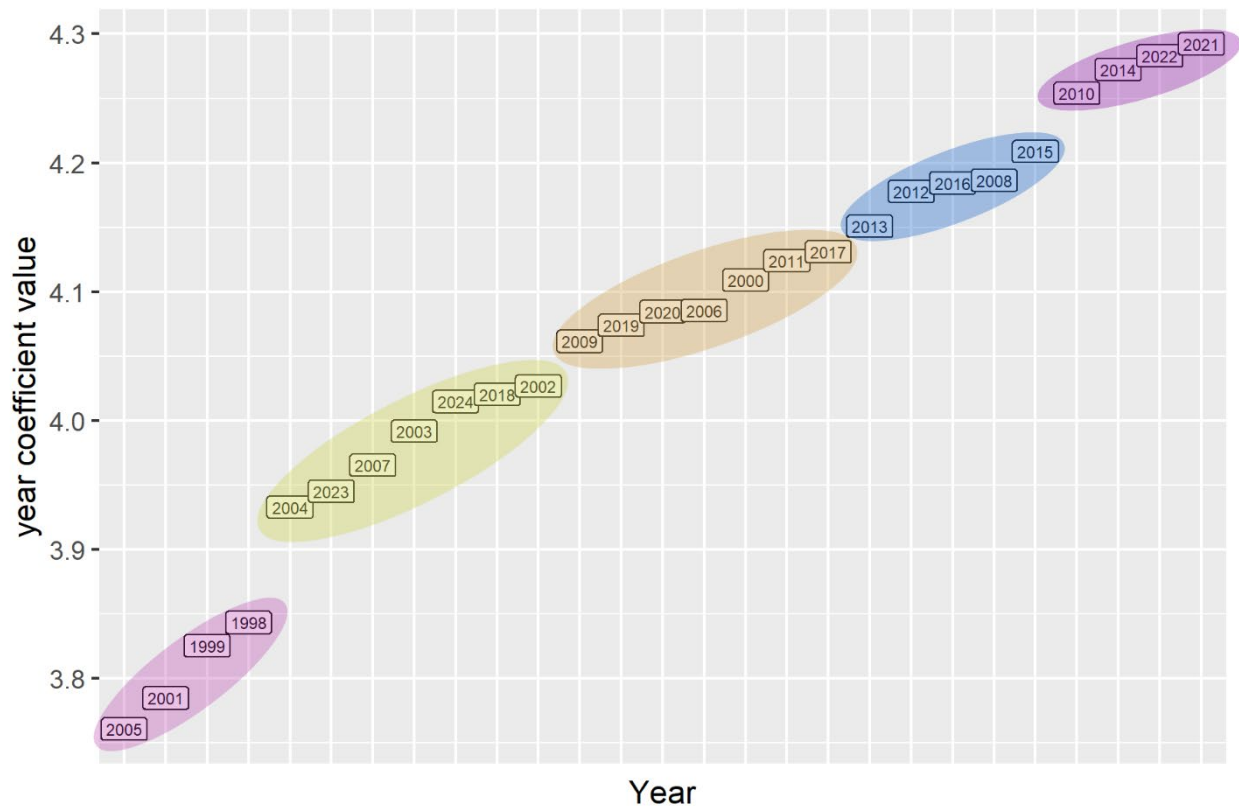


Figure 2. Survey years grouped by the similarity of their parameter coefficients into five blocks. Survey year was evaluated as a categorical covariate using multiple covariate distance sampling modeling. The coefficients for each year, calculated from modeling the effects of each year, were plotted in ascending order, then grouped based on the following thresholds: ≤ 3.9 (rose), >3.9 to ≤ 4.05 (yellow), >4.05 to ≤ 4.15 (amber), >4.15 to ≤ 4.25 (blue), and >4.25 (violet).

Density estimates (birds/km²) were calculated from point-transect distance sampling data using the R (R Core Team 2024) package *Distance* (version 1.0.9; Miller *et al.* 2019). Population abundance estimates were the product of the density estimate times the area of the core survey area (64.4 km²). The 2022–2024 data were pooled with detections from previous surveys since 1998. Candidate models were limited to half-normal and hazard-rate detection functions with expansion series of order two (361, 365; Buckland *et al.* 2001). Survey effort in a given year was adjusted by the number of times the station was counted in that year.

To improve model precision, potential sampling covariates were incorporated in the multiple covariate distance sampling engine of *Distance*. Covariates included the weather conditions, time of sampling, type of detection, and year of survey. The right-tail truncation for the 1998–2018 data was 87.5 m (Genz *et al.* 2018); the distance where the detection probability was 10% in the non-truncated model. The 10% truncation distance in this analysis was 90 m, which is a “heaping” distance (i.e., rounding of distances to favored values). Because Buckland *et al.* (2015) state that a heaping distance should not be selected as a truncation distance, we chose the previous truncation distance (Genz *et al.* 2022) of 87.5 m. Truncation facilitates modeling by deleting outliers and reducing the number of adjustment parameters needed to modify the detection function. The detection probability model selected was the one having the lowest Akaike’s information criterion (AIC; Buckland *et al.* 2001, Burnham and Anderson 2002). Visual inspection of diagnostic plots was conducted, and model fit was evaluated with a Cramr-von Mises test (Buckland *et al.* 2015). Annual population densities for each survey were calculated using the global detection function, and the pooled data were post-stratified by year and location (inside/outside core survey area). The 95% confidence intervals for the annual density estimates were derived from the 2.5th and 97.5th percentiles using bootstrap methods in *Distance* for 1,000 iterations (Buckland *et al.* 2001, Thomas *et al.* 2010).

Trend Detection

The trend in palila abundance was assessed in two different ways. First, the bootstrap sample estimates generated to evaluate uncertainty in population abundance were used to approximate the long-term population trend (1998–2024) with a log-linear regression model. We evaluated the trend over four time periods—the full modern time span of 26 years, the most recent 15 years, the most recent 10 years, and the most recent 5 years. The evidence of a trend was derived from the bootstrap distribution of slopes following Camp *et al.* (2015). Diagnostics demonstrated that the log-linear regressions of trends met model assumptions according to visual inspection of residual plots. Shapiro-Wilk normality test ($w = 0.90$, $P = 0.011$) for the complete 26-year time series indicated that the abundance estimates were not normally distributed, however the 15-, 10-, and 5-year timeseries estimates did have normal distributions. Temporal autocorrelation was evident across all four of the time series.

Because of the temporal autocorrelation, we also used a Bayesian state-space model on the log-scale, which provided an inherently auto-correlated alternative trends assessment. A state-space model separates model uncertainty into portions attributable to observation error (due to random noise in the environment affecting detectability and measurement) and process error (due to stochastic fluctuations in population outside of the overall trend). Such a state-space model can be interpreted as a biologically informed smoother and provides annual estimates consistent with the observed inter-annual noise. We used diffuse priors for the model parameters: a normal distribution with mean 0 and standard deviation of 10 for the annual mean population change and exponential priors with mean 0.1 as priors for the standard deviation of slope and the observation error.

The state-space model was fit using the *rjags* package (ver. 4-16; Plummer 2003), which uses a Markov chain Monte Carlo algorithm. The trends were centered on the mean bootstrap abundance estimate across the timeseries to improve model convergence. The model

parameters were estimated from 1,010,000 iterations for each of six chains (i.e., model runs) after first discarding 10,000 iterations as a “warm-up” period. The six chains were pooled (6,000,000 total iterations) to calculate the posterior distribution. Gelman-Rubin convergence statistics for all estimated parameters were well below 1.01, which is less than the 1.1 threshold that indicates convergence (Gelman and Rubin 1992).

Both methods were assessed in an equivalence-testing approach (Camp *et al.* 2008) using the observed distribution of slopes of the bootstrap distribution and the posterior distribution of the slopes from the Bayesian state-space model. We chose biologically meaningful thresholds for the overall population trend as a 25% change in the population over a 25-year period (annual rate of change equal to -0.0119 and 0.0093 [for decreasing and increasing] on the log-scale). A biologically meaningful trend occurs when the posterior probability distribution of the slope lies outside the equivalence region, whereas a negligible trend occurs when the slope is within the equivalence region. An inconclusive result occurs when small sample size and high variation in estimates results in the posterior distribution of the slope providing weak evidence in the three outcomes (increasing, stable, and decreasing). The strength of evidence for a trend was based on the distribution defined as weak, moderate, strong, or very strong based on the percentage of bootstrap slopes in each category: weak if <50%, moderate if between 50% and 70%, strong if between 70% and 90%, and very strong if >90%.

Sampling Condition Evaluation

The sampling conditions, particularly weather that could hinder or prohibit detecting birds, can adversely affect population estimates. We compared the distributions and probability densities of weather covariates by survey year using violin plots. Violin plots are similar to box plots in that they depict the summary statistics of mean, median, and interquartile ranges, but also display the full distribution of the data and include a kernel density to show structures in the data. Assessments were evaluated visually.

RESULTS

Abundance Estimation

Within the 64.4-km² core survey area of the southwestern flank of Mauna Kea, the number of palila detected decreased by 21.8% from 2021 to 2022 (101 in 2021 and 79 in 2022). There was a 38.0% decrease in detections between 2022 and 2023 (79 in 2022 and 49 in 2023) and a slight increase of 8.2% between 2023 and 2024 (49 in 2023 and 53 in 2024; Figure 3).

Due to the lower numbers of detections in 2022, 2023, and 2024, fewer covariates could be reliably modeled with sufficient sample size (at least 5 per level) post-stratification, resulting in a smaller set of candidate models (Table 2). This limited our ability to detect any effects from weather covariates or observers on detectability. For this reason, we inspected the distribution of weather covariate values to identify any clear outliers or patterns across survey years. The hazard-rate detection function model with year block as the covariate had the lowest AIC by more than 29 units (Table 2, Figure 4). Inspection of the diagnostic plots (probability detection function and probability density) indicated that the model adequately fit the data (Figure 4). The Cramér-von Mises test indicated that the detection function did not statistically differ from the distance histogram (test statistic = 0.43, $P = 0.060$, $\alpha = 0.05$). No palila were detected outside of the core survey area during annual counts between 2020 and 2024 (Table 3). In 2022, the palila population in the core survey area was estimated at 367–742 birds (point estimate: 545; Table 3, Figure 5). In 2023, the palila population in the core survey area was estimated at 374–842 birds (point estimate: 596). In 2024, the palila population in the core survey area was estimated at 412–970 birds (point estimate: 666).

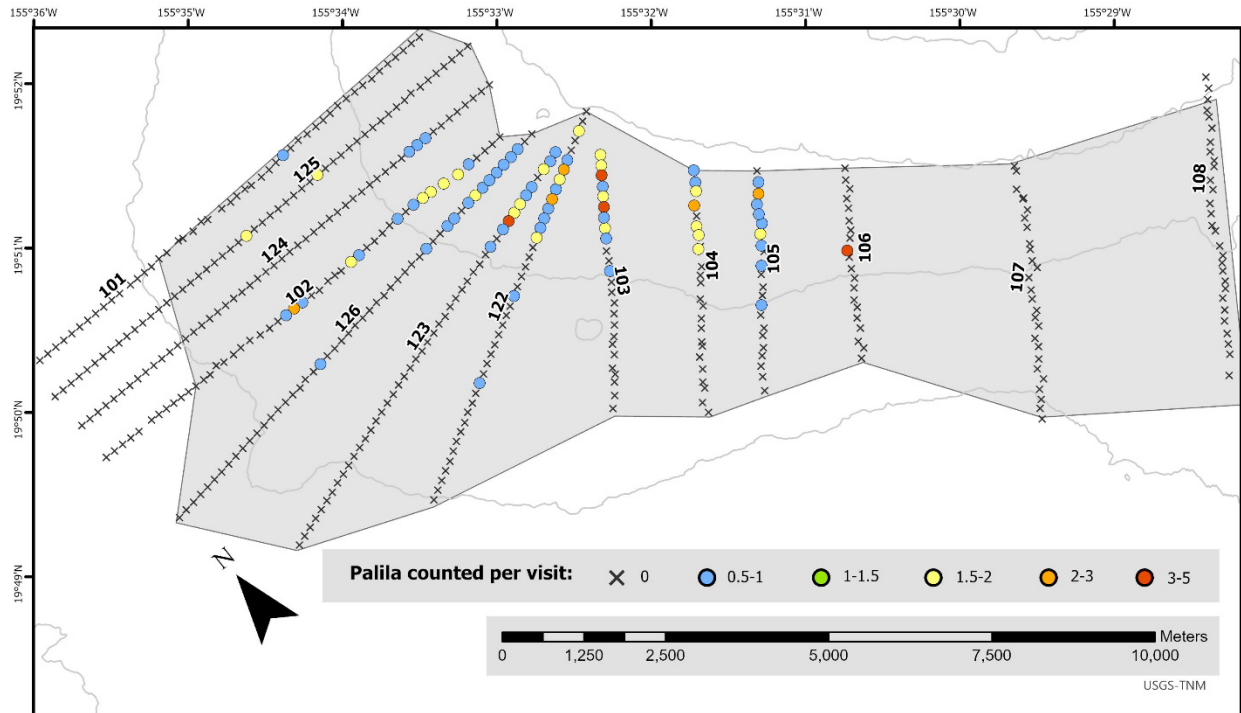


Figure 3. Palila detected per visit across 2022–2024 surveys. Stations surveyed more than once display mean numbers of detections. X symbols mark stations where no palila were detected during 2022–2024 surveys regardless of survey effort. The shaded region marks the area surveyed to estimate abundance, and transect numbers are included for reference to Figure 1. Graticule tick marks are provided to show geographic coordinates along the border. The map has been rotated to minimize white space. Base map from World Geodetic System 1984 (WGS84) zone 5 (U.S. Geological Survey 2018; contour interval 500 m).

Trend Detection

Between 1998 and 2005, palila numbers fluctuated moderately between 4,000 and 6,800 except for a dip in 2000 (Figure 5). After 2005, palila population estimates declined steadily through 2010. During 2014–2024, estimates fluctuated moderately (average CV = 0.14) with a local peak in 2019. The observed mean decline during 1998–2024 has been 203 birds per year. The bootstrap log-linear regression model showed very strong evidence (posterior probability $P = 1.0$) of a downward trend in palila abundance for all time periods examined. The log-linear state-space model (Figure 6) also shows very strong evidence of a decline with 100% posterior probability showing a downward trend for all four time series. The regression model fit with a Bayesian R^2 of 0.81. Figure 6 also shows downward trends for the last 5, 10, and 15 years. All three showed a 100% probability of the population declining.

Sampling Condition Evaluation

The 2021 abundance estimates are about half that of 2020 estimates. Similar to 2021, abundance estimates declined more than 35% in 2000, 2006, 2010, and 2015, immediately after which estimates increased, except in the case of 2006. Weather conditions during these surveys did not contribute to low estimates as they did not differ markedly from conditions during other surveys (Figure 7). This is because surveys were halted when sampling conditions hindered detecting birds (e.g., heavy rains or strong winds/gusts).

Table 2. Results of fitting 12 detection function models to the 1998–2024 palila distance histogram. Δ AIC is the difference in Akaike’s information criterion (AIC) scores between each model and the overall best-fit model, and w is the discrete model probability. The hazard-rate detection with blocks of years as a factor was chosen (bold) as the best model.

| Model ^{1,2} | Number of parameters | AIC | Δ AIC | w |
|---------------------------------|----------------------|-----------------|--------------|----------|
| H-rate key yearblock (f) | 6 | 50598.65 | 0 | 1 |
| H-rate key year (f) | 28 | 50628.30 | 29.6527 | 0 |
| H-rate key heard vs. seen | 3 | 50688.32 | 89.6659 | 0 |
| H-rate key gusty/not gusty | 3 | 50944.97 | 346.3213 | 0 |
| H-rate key windy/not windy | 3 | 50959.98 | 361.3285 | 0 |
| H-rate key simple polynomial | 3 | 50965.38 | 366.7301 | 0 |
| H-rate key | 2 | 50973.17 | 374.5157 | 0 |
| H-rate key mins since start | 3 | 50975.16 | 376.5107 | 0 |
| H-norm key | 1 | 51135.58 | 536.9275 | 0 |

¹Models are hazard-rate (H-rate) and half normal (H-norm) key detection functions; adjustment term is simple polynomial; and covariates are year (year; factor = f), and block year (yearblock; years pooled into 5 blocks based on parameter coefficients; factor = f), detection type heard only vs. seen (detection type 1 vs. 2 and 4 pooled), gust strength ≥ 2 (gusty) or < 2 (not gusty), wind strength ≥ 2 (windy) or < 2 (not windy), and minutes since earliest survey start time at detection.

²Models H-rate with cosine adjustment term and H-norm with cosine and Hermite polynomial adjustment terms failed to converge due to monotonicity issues and are not included in the table.

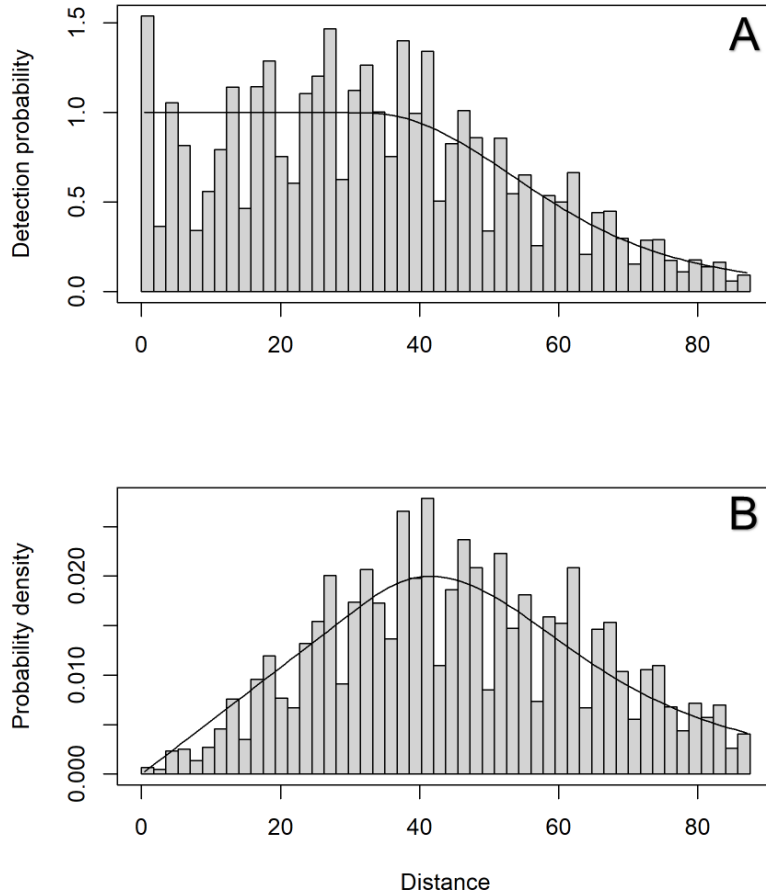


Figure 4. Hazard-rate detection function (A) and probability density (B) of the best-fit detection model. There are no expansion series, and blocked years is included as a detection covariate. The model was fit using palila distance (in meters) data pooled across all surveys from 1998 to 2024. Data were truncated at 87.5 m. Figure 4B shows how the observed probability distribution of distances (gray bars) matches the modeled detection function, especially at short distances.

Table 3. Annual palila detections and population estimate parameters from 1998–2024. Detections are given for palila recorded inside the core survey area and for stations outside the core survey area during six-minute counts. Population parameters include the population estimate, percent coefficient of variation (%CV), standard error (SE), and lower and upper limits of the 95% confidence interval inside the core survey area.

| Year | # Detections inside core survey area | # Detections outside core survey area | Estimate | % CV | SE | Lower limit | Upper limit |
|-------------------|--|---|----------|---------|-----|----------------|----------------|
| 1998 | 315 | 2 | 5,952 | 9.8 | 600 | 4,895 | 7,253 |
| 1999 | 389 | 0 | 6,822 | 9.4 | 649 | 5,693 | 8,167 |
| 2000 | 242 | 12 | 2,435 | 10.5 | 249 | 1,946 | 2,940 |
| 2001 | 331 | 4 | 5,918 | 10.9 | 620 | 4,732 | 7,196 |
| 2002 | 339 | 9 | 4,280 | 9.1 | 385 | 3,548 | 5,075 |
| 2003 | 442 | 4 | 5,487 | 8.2 | 463 | 4,593 | 6,459 |
| 2004 | 371 | 8 | 4,637 | 8.3 | 396 | 3,879 | 5,415 |
| 2005 | 315 | 0 | 5,460 | 9.4 | 541 | 4,412 | 6,566 |
| 2006 | 267 | 15 | 3,026 | 10.6 | 318 | 2,448 | 3,674 |
| 2007 | 210 | 3 | 2,736 | 9.5 | 284 | 2,230 | 3,306 |
| 2008 | 192 | 0 | 1,826 | 10.7 | 192 | 1,469 | 2,228 |
| 2009 | 187 | na | 1,919 | 13.3 | 227 | 1,490 | 2,357 |
| 2010 | 151 | na | 984 | 13.3 | 124 | 752 | 1,231 |
| 2011 | 119 | na | 1,060 | 12.5 | 147 | 785 | 1,376 |
| 2012 ¹ | 362 | 0 | 1,489 | 13.0 | 163 | 1,193 | 1,828 |
| 2013 ² | 337 | na | 1,219 | 10.5 | 114 | 1,002 | 1,450 |
| 2014 ³ | 351 | 4 | 1,250 | 10.5 | 121 | 1,032 | 1,498 |
| 2015 ⁴ | 192 | 1 | 776 | 16.7 | 99 | 589 | 976 |
| 2016 ⁵ | 319 | 4 | 1,346 | 9.5 | 154 | 1,065 | 1,664 |
| 2017 ⁶ | 248 | 9 | 1,196 | 10.5 | 142 | 937 | 1,480 |
| 2018 | 99 | 3 | 1,030 | 12.5 | 154 | 736 | 1,332 |
| 2019 | 146 | 4 | 1,436 | 18.2 | 230 | 1,034 | 1,944 |
| 2020 | 141 | 0 | 1,310 | 15.0 | 203 | 936 | 1,747 |
| 2021 | 101 | 0 | 679 | 18.2 | 130 | 444 | 956 |
| 2022 | 79 | 0 | 545 | 25.0 | 97 | 367 | 742 |
| 2023 | 49 | 0 | 596 | 22.2 | 122 | 374 | 842 |
| 2024 | 53 | 0 | 666 | 20.0 | 144 | 412 | 970 |

¹Of 362 total detections, 194 recorded on first count, 168 recorded on subsequent counts.

²Of 337 total detections, 178 recorded on first count, 159 recorded on subsequent counts.

³Of 351 total detections, 163 recorded on first count, 188 recorded on subsequent counts.

⁴Of 192 total detections, 99 recorded on first count, 93 recorded on subsequent counts.

⁵Of 319 total detections, 178 recorded on first count, 141 recorded on subsequent counts.

⁶Of 248 total detections, 138 recorded on first count, 110 recorded on subsequent counts.

na = outside core survey area was not surveyed

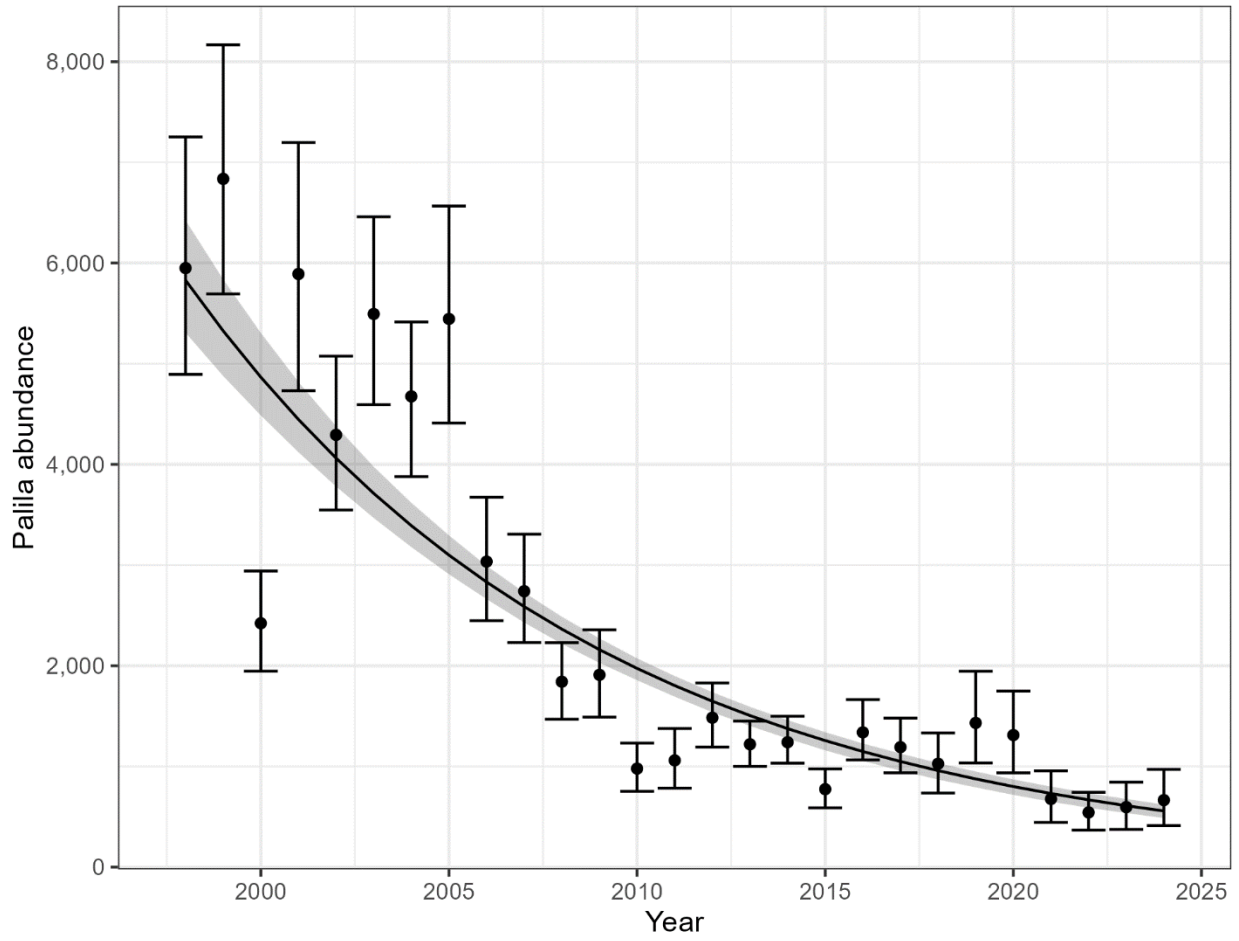


Figure 5. Annual palila population estimates from 1998 through 2024 inside the core survey area on the western slope of Mauna Kea. The line represents the best fit log-linear regression, error bars show 95% bootstrap intervals around the point estimates, and the shaded area shows the 95% band around the bootstrapped regression.

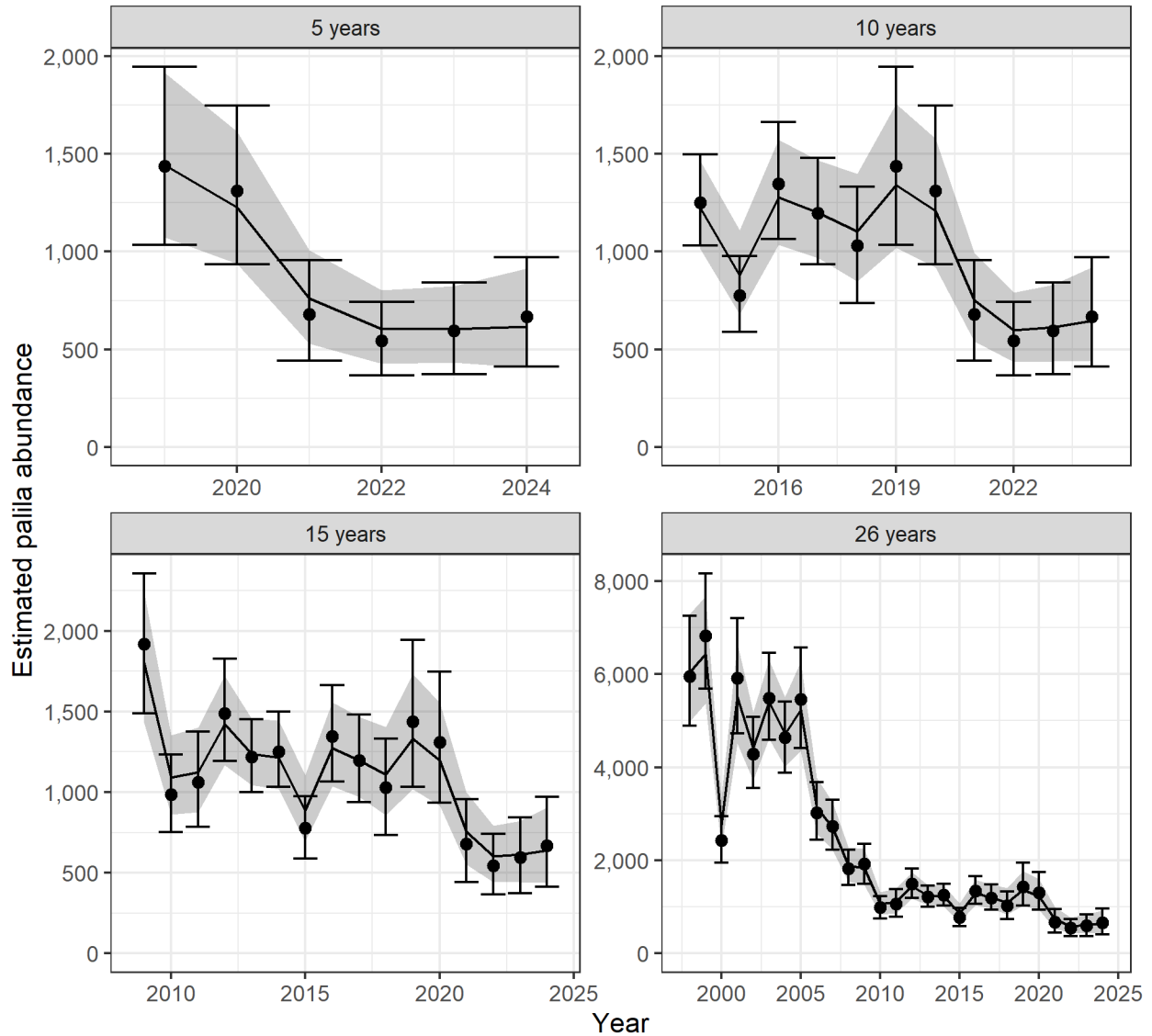


Figure 6. State-space model estimates of palila abundance over multiple time spans—the most recent 5, 10, and 15 years, and the full series from 1998 to 2024 (26-year monitoring period). Points and error bars are estimates from *Distance* models. The lines show the median estimate from the Bayesian posterior distribution of abundance, and the shaded error shows the 95% credible interval of abundance posteriors.

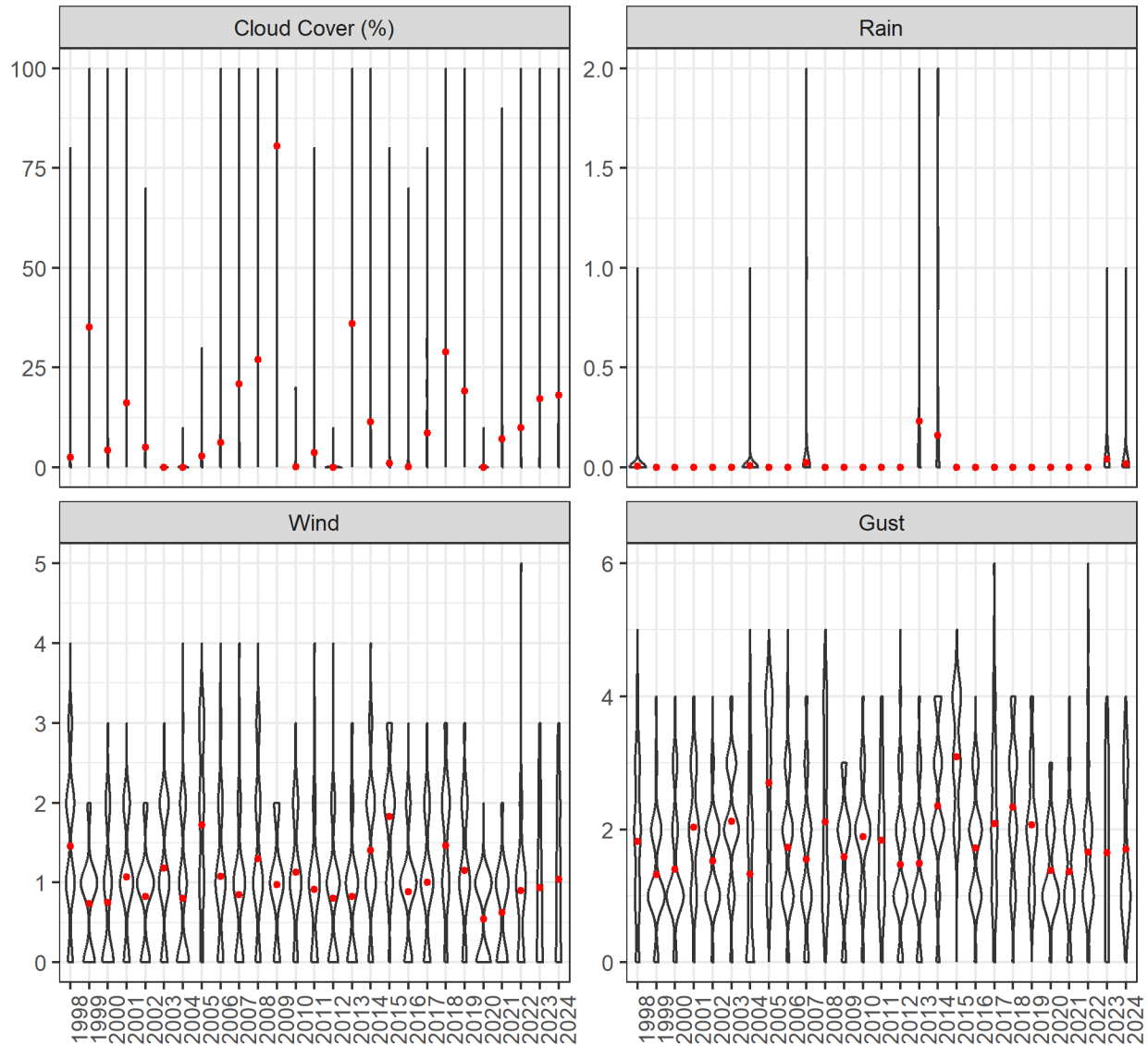


Figure 7. Violin plots displaying the distribution of weather covariate values for each survey year. The thickness of the density curve represents the frequency of a numerical value for each year. Red dots depict the mean value at each year. Cloud cover was recorded at the nearest 10%, whereas all other covariates were recorded on discrete numerical scales. Rain values were recorded as categories between 0 and 4, with 0 equaling no rain and 4 equaling heavy rain. Wind speed was recorded on the Beaufort scale from 0 to 5, with 0 equaling calm conditions and 5 equaling strong breeze. Gust is the maximum wind speed and was also recorded on the Beaufort scale.

CONCLUSIONS

The palila population hit an all-time low of 367–742 birds (point estimate: 545) in 2022. The population increased in 2023 to 374–842 birds (point estimate: 596), and further to 412–970 birds (point estimate of 666) in 2024. However, there was very strong evidence that the palila population has declined since the current survey transects were implemented in 1998. Table 3 and Figure 5 show the population fluctuating in the 4,000–6,800 range (except in 2000) from

1998 to 2005, at which point a steep decline began. Beginning around 2010 the steep decline appears to level off (around an abundance of 1,000), but the trend assessments show the population continues to decline, leading to a record low in 2022.

The mean decline during 1998–2024 was 203 birds per year, resulting in a >90% decline in the population over the 26-year monitoring period. In this report we produced trend assessments for a range of time spans to examine how different time periods might affect conclusions. In strict practice the time frame for a trend assessment is best determined before the data are analyzed to avoid post-facto choices to arrive at a desired conclusion, so for our purposes the trend across the full 26-year span is definitive. Figure 5 shows that different trends (possibly due to different population dynamics or environmental effects) are operating in the 1998–2024 time span. Future analyses may wish to specify an assessment beginning after the decline seems to have leveled off, or for the previous 10 years, to measure the effect of current population and environmental conditions.

The palila population is almost certainly continuing to decline. The most optimistic method (state-space assessment for the most recent 10 years) shows a 0% chance of the trend being stable or upward. Based on the methods used and estimates reported in Johnson *et al.* (2006), the estimated abundance of palila in 2022 was the lowest since regular surveys began in 1980.

Abnormally low estimates, as in 2000, 2006, 2010, and 2015, which appear biologically unlikely, can sometimes be an artifact of differences between detection probability related to environmental conditions or surveying effort. As palila detections became fewer in number over the last two decades, our ability to reliably model weather conditions as covariates diminished. However, based on plots of their distributions, weather conditions in 2000 were not markedly different from those of previous surveys, nor were the conditions different during other years when estimates were low (Figure 7). Therefore, weather conditions were not likely to contribute to the low estimates. Likewise, survey effort did not differ markedly between these low years and their adjacent years (Table 1). The low estimate of 1,946 to 2,940 birds (point estimate 2,435) in 2000 is most likely an outlier representing sampling error as the population then doubles or triples to 4,732 to 7,196 birds (point estimate 5,918) in 2001. However, unlike the 2000 estimate, the 2021 and 2022 estimates were followed by similarly low estimates in 2023 and 2024 which overlap their confidence intervals, and therefore, we think this represents a true population decline.

In the 2017 mountain-wide survey, no palila were detected along the southeastern and eastern slopes of Mauna Kea, where they have been detected historically, but there were two detections on the north slope, where wild birds were translocated (1997–1998, 2004–2006), and captive-reared birds were released (2003–2005, 2009 [Banko and Farmer 2014], and 2019 [Matsuoka *et al.* 2021]). Palila have not been detected outside the core survey area at lower elevation during annual surveys since 2019. However, previous detections suggest that they may use former pasture lands that have been removed from grazing and subject to reforestation implemented through the Mauna Kea Forest Restoration Project (dlnr.hawaii.gov/restoremaunakea/). Reducing the added impacts of other major limiting factors affecting palila, particularly predation, could be important for the long-term survival of this species.

ACKNOWLEDGEMENTS

Support for the annual palila surveys since 1998 was provided by the Federal Highway Administration, U.S. Army Garrison Hawaii, Hawaii Department of Land and Natural Resources (DLNR) Division of Forestry and Wildlife, U.S. Fish and Wildlife Service State Wildlife Grant

Program, American Bird Conservancy, National Fish and Wildlife Foundation, and the U.S. Geological Survey Wildlife Program. Funding for analyses of the data since 2012 was provided by the Hawaii DLNR Division of Forestry and Wildlife. We are grateful to the many agency staff and volunteers who helped collect survey data. We thank Colleen Cole and James Jacobi for providing technical peer review that improved the manuscript. Editorial and online publishing support provided by Sarah Nash, Hawai'i Cooperative Studies Unit. Data and metadata associated with this report from 1998 to 2018 are available at <https://doi.org/10.5066/P9DO0PL4> (Brink *et al.* 2022) and data from 2022 to 2024 are available from the DLNR upon request.

LITERATURE CITED

- Banko, P. C., and C. Farmer (editors). 2014. Palila restoration research, 1996–2012. Hawai'i Cooperative Studies Unit Technical Report HCSU-046. University of Hawai'i at Hilo, Hawaii, USA. 499 pp.
- Banko, P. C., K. W. Brinck, C. Farmer, and S. C. Hess. 2009. Recovery programs: palila. Chapter 23, pp. 513–529 *in* T. K. Pratt, C. T. Atkinson, P. C. Banko, J. D. Jacobi, and B. L. Woodworth (editors). Conservation Biology of Hawaiian Forest Birds: Implications for Island Avifauna. Yale University Press, New Haven, Connecticut, USA.
- Banko, P. C., L. Johnson, G. D. Lindsey, S. G. Fancy, T. K. Pratt, J. D. Jacobi, and W. E. Banko. 2020. Palila (*Loxioides bailleui*), version 1.0. *In* A. F. Poole and F. B. Gill (editors). Birds of the World. Cornell Lab of Ornithology, Ithaca, New York, USA. <https://doi.org/10.2173/bow.palila.01>
- Banko, P. C., M. L. Cipollini, G. W. Breton, E. Paulk, M. Wink, and I. Izhaki. 2002a. Seed chemistry of *Sophora chrysophylla* (mamane) in relation to the diet of the specialist seed predator *Loxioides bailleui* (palila) in Hawaii. *Journal of Chemical Ecology* 28:1389–1406.
- Banko, P. C., P. T. Oboyski, J. W. Slotterback, S. J. Dougill, D. M. Goltz, L. Johnson, M. E. Laut, and C. Murray. 2002b. Availability of food resources, distribution of invasive species, and conservation of a Hawaiian bird along a gradient of elevation. *Journal of Biogeography* 29:789–808. <https://doi.org/10.1046/j.1365-2699.2002.00724.x>
- Banko, P. C., R. J. Camp, C. Farmer, K. W. Brinck, D. L. Leonard, and R. M. Stephens. 2013. Response of palila and other subalpine Hawaiian forest bird species to prolonged drought and habitat degradation by feral ungulates. *Biological Conservation* 157:70–77.
- Banko, P. C., S. C. Hess, P. G. Scowcroft, C. Farmer, J. D. Jacobi, R. M. Stephens, R. J. Camp, D. L. Leonard Jr., K. W. Brinck, J. O. Juvik, and S. P. Juvik. 2014. Evaluating the long-term management of introduced ungulates to protect the palila, an endangered bird, and its critical habitat in subalpine forest of Mauna Kea, Hawai'i. *Arctic, Antarctic, and Alpine Research* 46(4):871–889. <https://doi.org/10.1657/1938-4246-46.4.871>
- Brinck, K. W., A. S. Genz, and R. J. Camp. 2022. Mauna Kea palila point count data from annual surveys 1998–2018 (ver. 2.0, January 2022): U.S. Geological Survey data release. <https://doi.org/10.5066/P9DO0PL4>
- Buckland, S. T., D. R. Anderson, K. P. Burnham, J. L. Laake, D. L. Borchers, and L. Thomas. 2001. Introduction to distance sampling: Estimating abundance of biological populations. Oxford University Press, Oxford, UK. 448 pp.

- Buckland, S. T., E. A. Rexstad, T. A. Marques, and C. S. Oedekoven. 2015. Distance sampling: Methods and applications. Springer International Publishing, Cham, Switzerland. 277 pp. <https://doi.org/10.1007/978-3-319-19219-2>
- Burney, D. A., H. F. James, L. P. Burney, S. L. Olson, W. Kikuchi, W. L. Wagner, M. Burney, D. McCloskey, D. Kikuchi, F. V. Grady, R. Gage, and R. Nishek. 2001. Fossil evidence for a diverse biota from Kaua'i and its transformation since human arrival. *Ecological Monographs* 71:615–641. [https://doi.org/10.1890/0012-9615\(2001\)071\[0615:FEFADB\]2.0.CO;2](https://doi.org/10.1890/0012-9615(2001)071[0615:FEFADB]2.0.CO;2)
- Burnham, K. P., and D. R. Anderson. 2002. Model selection and multimodel inference: A practical information-theoretic approach. Second edition. Springer-Verlag, New York, New York, USA.
- Camp, R. J., M. Gorresen, T. K. Pratt, and B. L. Woodworth. 2009. Population trends of native Hawaiian forest birds: 1976–2008. Hawai'i Cooperative Studies Unit Technical Report HCSU-012. University of Hawai'i at Hilo, Hawaii, USA. <https://hdl.handle.net/10790/2692>
- Camp, R. J., N. E. Seavy, P. M. Gorresen, and M. H. Reynolds. 2008. A statistical test to show negligible trend: Comment. *Ecology* 89:1469–1472. <https://www.jstor.org/stable/27651690>
- Camp, R. J., K. W. Brinck, and P. C. Banko. 2014. Palila abundance estimates and trend. Hawai'i Cooperative Studies Unit Technical Report HCSU-053. University of Hawai'i at Hilo, Hawaii, USA. <https://hdl.handle.net/10790/2611>
- Camp, R. J., K. W. Brinck, and P. C. Banko. 2016. 2015–2016 Palila abundance estimates. Hawai'i Cooperative Studies Unit Technical Report HCSU-076. University of Hawai'i at Hilo, Hawaii, USA. <https://hdl.handle.net/10790/2750>
- Camp, R. J., K. W. Brinck, P. M. Gorresen, F. A. Amidon, P. M. Radley, S. P. Berkowitz, and P. C. Banko. 2015. Current land bird distribution and trends in population abundance between 1982 and 2012 on Rota, Mariana Islands. *Journal of Fish and Wildlife Management* 6(2). <https://doi.org/10.3996/112014-JFWM-085>
- Camp, R. J., and P. C. Banko. 2012. Palila abundance estimates and trend. Hawai'i Cooperative Studies Unit Technical Report HCSU-033. University of Hawai'i at Hilo, Hawaii, USA. <https://hdl.handle.net/10790/2630>
- D'Antonio, C. M., and P. M. Vitousek. 1992. Biological invasions by exotic grasses, the grass/fire cycle, and global change. *Annual Review of Ecology, Evolution, and Systematics* 23:63–87. <https://www.jstor.org/stable/2097282>
- Gardner, D. E., and E. E. Trujillo. 2001. Association of *Armillaria mellea* with mamane decline at Pu'u La'au. *Newsletter of the Hawaiian Botanical Society* 40:33–34.
- Gelman, A., and D. B. Rubin. 1992. Inference from iterative simulation using multiple sequences. *Statistical Science* 7:457–511. <https://doi.org/10.1214/ss/1177011136>
- Genz, A. S., K. W. Brinck, C. K. Asing, L. Berry, R. J. Camp, and P. C. Banko. 2022. 2019–2021 Palila abundance estimates and trend. Hawai'i Cooperative Studies Unit Technical Report HCSU-101. University of Hawai'i at Hilo, Hawaii, USA. 20 pp. <https://hdl.handle.net/10790/6858>
- Genz, A. S., K. W. Brinck, R. J. Camp, and P. C. Banko. 2018. 2017–2018 Palila abundance estimates and trend. Hawai'i Cooperative Studies Unit Technical Report HCSU-086. University of Hawai'i at Hilo, Hawaii, USA. <https://hdl.handle.net/10790/4431>

- Gorresen, P. M., R. J. Camp, M. H. Reynolds, T. K. Pratt, and B. L. Woodworth. 2009. Status and trends of native Hawaiian songbirds. Chapter 5, pp. 108–136 *in* T. K. Pratt, C. T. Atkinson, P. C. Banko, J. D. Jacobi, B. L. Woodworth (editors). *Conservation biology of Hawaiian forest birds: Implications for island avifauna*. Yale University Press, New Haven, Connecticut, USA.
- Gray, E. M., P. C. Banko, S. J. Dougill, D. Goltz, L. Johnson, M. E. Laut, J. D. Semones, and M. R. Wiley. 1999. Breeding and nonbreeding censuses of the 1998 palila population on Mauna Kea, Hawai'i. *'Elepaio* 59:33–39.
- Hess, S. C., P. C. Banko, D. M. Goltz, R. M. Danner, and K. W. Brinck. 2004. Strategies for reducing feral cat threats to endangered Hawaiian birds. *In* *Proceedings of the Vertebrate Pest Conference* 21:21–26.
- Hess, S. C., P. C. Banko, G. J. Brenner, and J. D. Jacobi. 1999. Factors related to the recovery of subalpine woodland on Mauna Kea, Hawaii. *Biotropica* 31:212–219. <https://doi.org/10.1111/j.1744-7429.1999.tb00133.x>
- Hess, S. C., P. C. Banko, M. H. Reynolds, G. J. Brenner, and L. P. Laniawe. 2001. Seasonal changes in food resource abundance and drepanidine densities in subalpine woodland on Mauna Kea, Hawai'i. *Studies in Avian Biology* 22:154–163.
- Hughes, F., P. M. Vitousek, and T. Tunison. 1991. Alien grass invasion and fire in the seasonal submontane zone of Hawai'i. *Ecology* 72:743–746. <https://doi.org/10.2307/2937215>
- Jacobi, J. D., S. G. Fancy, J. G. Giffin, and J. M. Scott. 1996. Long-term population variability in the palila, an endangered Hawaiian honeycreeper. *Pacific Science* 50:363–370.
- Johnson, L., R. J. Camp, K. W. Brinck, and P. C. Banko. 2006. Long-term population monitoring: lessons learned from an endangered passerine in Hawai'i. *Wildlife Society Bulletin* 34:1055–1063. [https://doi.org/10.2193/0091-7648\(2006\)34\[1055:LPMLLF\]2.0.CO;2](https://doi.org/10.2193/0091-7648(2006)34[1055:LPMLLF]2.0.CO;2)
- Juvik, J. O., and S. P. Juvik. 1984. Mauna Kea and the myth of multiple use. *Mountain Research and Development* 4:191–202. <https://doi.org/10.2307/3673140>
- Leonard, Jr., D. L., P. C. Banko, K. W. Brinck, C. Farmer, and R. J. Camp. 2008. Recent surveys indicate rapid decline of palila population. *'Elepaio* 68:27–30.
- Lerner, H. R., M. Meyer, H. F. James, M. Hofreiter, and R. C. Fleischer. 2011. Multilocus resolution of phylogeny and timescale in the extant adaptive radiation of Hawaiian honeycreepers. *Current Biology* 21:1838–1844. <https://dx.doi.org/10.1016/j.cub.2011.09.039>
- Lindsey, G. D., T. K. Pratt, M. H. Reynolds, and J. D. Jacobi. 1997. Response of six species of Hawaiian forest birds to a 1991–1992 El Niño drought. *The Wilson Bulletin* 109:339–343. <https://www.jstor.org/stable/4163820>
- Matsuoka, K., J. Tupu, A. Lilly, A. Bischer, L. Berry, J. Gaudioso-Levita, A. Wang, K. Asing, K. Brinck, and B. Masuda. 2021. Palila release 2019 summary. Unpublished report to the Palila Hui, a joint working group of the U.S. Fish and Wildlife Service, American Bird Conservancy, Hawaii Department of Land and Natural Resources-Division of Forestry and Wildlife, San Diego Zoo Wildlife Alliance, University of Hawai'i-Pacific Cooperative Studies Unit, and U.S. Geological Survey.
- Miller, D. L., E. Rexstad, L. Thomas, L. Marshall, and J. L. Laake. 2019. Distance sampling in R. *Journal of Statistical Software* 89:1–28. <https://doi.org/10.18637/jss.v089.i01>

- Oboyski, P. T., J. W. Slotterback, and P. C. Banko. 2004. Differential parasitism of seed-feeding *Cydia* (Lepidoptera: Tortricidae) by native and alien wasp species relative to elevation in subalpine *Sophora* (Fabaceae) forests on Mauna Kea, Hawaii. *Journal of Insect Conservation* 8:229–240. <https://digitalcommons.unl.edu/usgsstaffpub/634>
- Olson, S. L., and H. F. James. 1982. Prodrromus of the fossil avifauna of the Hawaiian Islands. Smithsonian Contributions to Zoology No. 365. Washington, DC, USA.
- Plummer, M. 2003. JAGS: A program for analysis of Bayesian graphical models using Gibbs sampling. *In* Proceedings of the 3rd international workshop on distributed statistical computing 124:1–10.
- R Core Team. 2024. R: A language and environment for statistical computing. R Foundation for Statistical Computing, Vienna, Austria. <https://www.R-project.org/>
- Reddy, E., D. H. Van Vuren, P. G. Scowcroft, J. B. Kauffman, and L. Perry. 2012. Long-term response of the mamane forest to feral herbivore management on Mauna Kea, Hawaii. *Pacific Conservation Biology* 18:123–132. <https://doi.org/10.1071/PC120123>
- Scott, J. M., S. Mountainspring, C. van Riper III, C. B. Kepler, J. D. Jacobi, T. A. Burr, and J. G. Giffin. 1984. Annual variation in the distribution, abundance, and habitat response of the palila (*Loxioides bailleui*). *Auk* 101:647–664. <https://doi.org/10.2307/4086892>
- Scowcroft, P. G. 1983. Tree cover changes in mamane (*Sophora chrysophylla*) forests grazed by sheep and cattle. *Pacific Science* 37:109–119.
- Thomas, L., S. T. Buckland, E. A. Rextad, J. L. Laake, S. Strindberg, S. L. Hedley, J. R. B. Bishop, T. A. Marques, and K. P. Burnham. 2010. Distance software: Design and analysis of distance sampling surveys for estimating population size. *Journal of Applied Ecology* 47:5–14. <https://doi.org/10.1111/j.1365-2664.2009.01737.x>
- U.S. Fish and Wildlife Service (USFWS). 2006. Revised recovery plan for the Hawaiian forest birds. U.S. Fish and Wildlife Service, Region 1, Portland, Oregon, USA.
- U.S. Geological Survey. 2018. National elevation dataset (NED): U.S. Geological Survey database. <https://www.usgs.gov/publications/national-elevation-dataset>, accessed 4 April 2025.
- Van Houtan, K. S., T. O. Gagné, P. Banko, M. E. Hagemann, R. W. Peck, and C. T. Yarnes. 2024. Climatic drought and trophic disruption in an endemic subalpine Hawaiian forest bird. *Biological Conservation* 299, 110823. <https://doi.org/10.1016/j.biocon.2024.110823>